Ultrahigh-resolution photoluminescence studies of excitons bound to boron in silicon under uniaxial stress

V. A. Karasyuk,* A. G. Steele,† Alison Mainwood
E. C. Lightowlers, and Gordon Davies
Physics Department, King's College London, Strand, London WC2R 2LS, United Kingdom

D. M. Brake and M. L. W. Thewalt
Department of Physics, Simon Fraser University, Burnaby, British Columbia, Canada V5A 1S6
(Received 23 December 1991)

The effects of uniaxial stress on the no-phonon photoluminescence spectrum of the boron bound exciton in silicon have been investigated using ultrahigh-resolution Fourier-transform spectroscopy. Under stresses of 0 to 25 MPa, in the ⟨001⟩, ⟨110⟩, and ⟨111⟩ directions, up to 25 components with linewidths of less than 10 μeV have been resolved. A theoretical model, extending the shell model, has been developed to interpret the splittings in the bound-exciton energy levels. This includes terms expressing electron-stress, hole-stress, electron-hole, hole-hole, and valley-orbit interactions, with spherical and anisotropic corrections. The model fits the experimental data very closely, and gives values for the magnitude of the interactions.

I. INTRODUCTION

Since the original discovery[1] of photoluminescence (PL) due to the recombination of donor and acceptor bound excitons (BE), silicon has remained the prototypical material for the study of BE in indirect band-gap hosts. Early studies[2] demonstrated that PL spectroscopy could provide a chemical identification of the various donor and acceptor species, which has led to the development of PL as a quantitative impurity characterization method for Si.[3–6]

A doublet splitting of the BE ground state for the acceptors B, Al, Ga, and In was reported in an early absorption measurement by Dean *et al.*[7] This structure was studied in more detail by Vouk and Lightowlers[8] using PL, which revealed a doublet structure for Al, Ga, and In, a triplet structure for Tl, the deepest single acceptor in Si, and no structure for the B BE.[8] The incorrect attribution of a doublet structure to the B BE by Dean *et al.*[7] was explained by Vouk and Lightowlers[8] as being due to a weak LO-phonon replica of the B BE line lying near the stronger TO-phonon replica. The B BE has a very weak no-phonon (NP) transition, and so in the earlier investigations was always studied in the TO-phonon-assisted region, even though this entailed the disadvantage of a phonon-related spectral broadening of the transition.[9]

Vouk and Lightowlers[8] proposed three possible explanations for the observed splittings, all of which involved hole-hole coupling between the two holes of the acceptor BE, but could not discriminate between these models based on the available data. The study of excitonic systems in Si received a great impetus upon the discovery[10–12] of bound multiexciton complexes (BMEC's) and the ensuing controversy over their existence.[13,14] In particular, it was recognized by a number of researchers that the structure of the acceptor ground state could be used to test the validity of the BMEC hypothesis, since the two-exciton acceptor BMEC should decay to the BE ground state, and therefore mirror the BE structure. This predicted effect was soon observed, and in addition the ground states of the Al and Ga BE were further resolved into triplets.[15–17]

Kirczenow[18] then demonstrated that the relative intensities of the triplet components were well accounted for by a simple hole-hole coupling model which neglected any electron-hole or electron valley-orbit effects. In this model, the two indistinguishable holes move in the field of the acceptor ion, which has T_d symmetry, and are described by the representations Γ_8 in the notation of Koster *et al.*[19] The hole-hole splitting is given by the antisymmetric product $\{\Gamma_8 \times \Gamma_8\} = \Gamma_1 + \Gamma_3 + \Gamma_5$. The relative intensities of the triplet lines suggested that the ordering was Γ_1, Γ_5, Γ_3 with Γ_1 lying lowest in energy. This assignment was supported by later uniaxial stress and Zeeman studies on BE and BMEC's associated with Al in Si.[20]

The case of the acceptor BE, with its large hole-hole splitting, was an explicit exception to the shell model (SM) introduced by Kirczenow[18] to explain the systematics of BE and BMEC spectra. In the SM the electrons (e) and holes (h) of the complex are placed, subject to the exclusion principle, in noninteracting single-particle states of donors and acceptors, respectively. Thus the SM neglected the possible splittings arising from e-e and e-h interactions. Hole-hole interactions, except for the acceptor BE, were also ignored as being too small to affect the overall structure of the BE and BMEC spectra. The advent of the SM led to considerable experimental activity, and in particular to numerous efforts to test its predictions using uniaxial stress and Zeeman splitting.[20–23] It was concluded[14] that the SM did a remarkably good job of explaining the structure of BE and BMEC spectra on

the resolution scale then available, which apart from the acceptor BE could not reveal the fine structure resulting from interactions between particles.

An attempt to measure the fine structure in the BE and BMEC PL spectra which might result from such interactions was made by Parsons,[24] who used a high-resolution scanning Fabry-Pérot interferometer in tandem with a grating spectrometer. He observed fine structure on several of the BMEC transitions associated with the donor P, and postulated their possible origins. The Fabry-Pérot method was perfected by Kaminskii, Karasyuk, and Pokrovskii,[25,26] who used it to study not only the fine structure but also the effects of uniaxial stress and magnetic fields on that structure.

In a more recent study the same technique was used to reveal fine structure in the lowest-energy (Γ_1) component of the BE luminescence associated with Al, Ga, and In acceptor BE's.[27] Since the electron in the BE cannot couple to the Γ_1 two-hole state to produce a splitting, the fine structure was ascribed to an electron valley-orbit splitting into Γ_1, Γ_3, and Γ_5 states. It was unfortunately not possible to search for similar fine structure on the transitions from the Γ_5 and Γ_3 two-hole states, since at temperatures high enough for these states to be thermally populated, a severe broadening occurs which probably results from very rapid transitions between the BE levels.[28]

This left the B acceptor BE as the only possibility for a complete study of the BE fine structure, since B with its repulsive central cell potential has a much smaller BE hole-hole splitting than does Al or Ga. As a result, all the BE initial states can be populated even at pumped He temperatures, and the thermal broadening may be less. Early evidence for structure in the B BE PL was a poorly resolved triplet seen with dispersive spectroscopy.[29] Later results using the Fabry-Pérot interferometer revealed additional fine structure, albeit still poorly resolved.[30]

More recently, it has been demonstrated that Fourier-transform PL spectroscopy using a Michelson interferometer can considerably surpass the results obtained by Fabry-Pérot interferometery, both in terms of spectral resolution and signal-to-noise ratio.[31,32] In particular, the B BE spectrum was found to consist of nine well-resolved components spanning an energy range of ~210 μeV.[32] This immediately suggested a scheme in which each of the three states arising from the hole-hole coupling was further split into three sublevels due to the valley-orbit splitting, with *e-h* interactions being negligible. It is the purpose of this paper to study the fine structure of the B BE using extremely homogeneous uniaxial stress along the ⟨001⟩, ⟨110⟩, and ⟨111⟩ directions, and by modeling the results, to arrive at a more complete description of the ground state of an indirect BE.

II. EXPERIMENTAL TECHNIQUES

The samples were cut from x-ray-oriented float-zone silicon with a boron concentration of 3×10^{15} cm^{-3}, in the shape of a parallelopiped $2 \times 2 \times 25$ mm^3 with pyramidal ends. They were mechanically polished, given a short etch in HNO_3-HF (10:1), and installed in the stress rig so that the ends of the pyramids matched small conical holes stamped in the exact centers of the ends of the stainless-steel pistons. Such a technique[26] allows precise orientation of the sample with respect to the applied force, giving a very uniform stress at the center of the sample.

The sample was immersed in a liquid-helium bath, at a temperature of either 4.2 or 2 K, and excited by a focused Ti-sapphire laser beam at 0.3 W cw, tuned to a wavelength of 0.92 μm. Luminescence spectra were recorded with a BOMEM DA3.01 Fourier-transform spectrometer using a cooled InGaAs photodiode. The stress in the samples was measured precisely by calibrating it against the linear splitting of the phosphorus BE line,[23,33] which itself was measured carefully in samples doped with 5×10^{14} cm^{-3} of phosphorus. By very careful selection of the material for the samples, and the highly precise techniques described, we were able to obtain spectra with a resolution of 3 μeV, and an inhomogeneous stress broadening of the lines of less than 10 μeV, for uniaxial stresses of up to 20 MPa.

III. RESULTS

The photoluminescence spectrum of the no-phonon (NP) boron BE transition is shown in Fig. 1. It consists of nine well-resolved components, with linewidths of about 10 μeV. Since the final state of the transition is

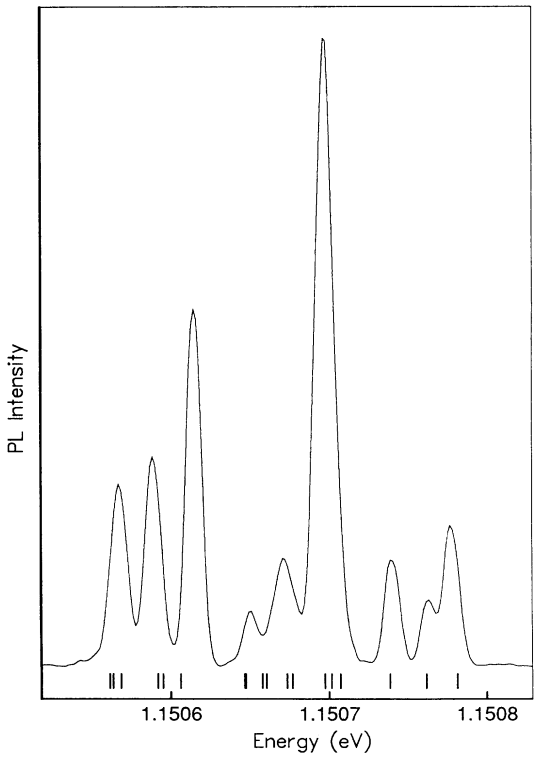

FIG. 1. Boron BE no-phonon photoluminescence spectrum with a resolution of 3 μeV, at 2 K, with no stress. Vertical ticks show theoretical predictions of the line energies.

the ground state of the boron acceptor, which has no fine structure, the spectral splitting is a direct representation of the energy levels of the initial state, that is, of the BE.

The evolution of the BE spectra under uniaxial compression is shown in Fig. 2 (for moderate stress) and Fig. 3 (for some of the highest stresses used here). These spectra have been obtained using nominally unpolarized luminescence. For ⟨001⟩ stress (the bottom part of Fig. 3), we show spectra recorded at 4.2 as well as 2 K. Considerable changes occur in the relative intensities of the lines, especially with the thermal population of the higher-energy states.

From the energies of all the observed stress-split components for each direction of stress, the boron BE energy levels are calculated by adding or subtracting half the observed stress splitting of the boron acceptor, depending on the final state ($m_j = \pm\frac{3}{2}$ or $m_j = \pm\frac{1}{2}$, respectively). The boron BE energies are shown by the points on Fig. 4. The lines are calculated using the theory of Secs. IV and V.

Additional data on the transitions were obtained by measuring their linear polarization. Figure 5 shows spectra recorded with polarization parallel and perpendicular to the applied ⟨001⟩ stress. They are compared with theoretical spectra calculated as described in Secs. IV and V.

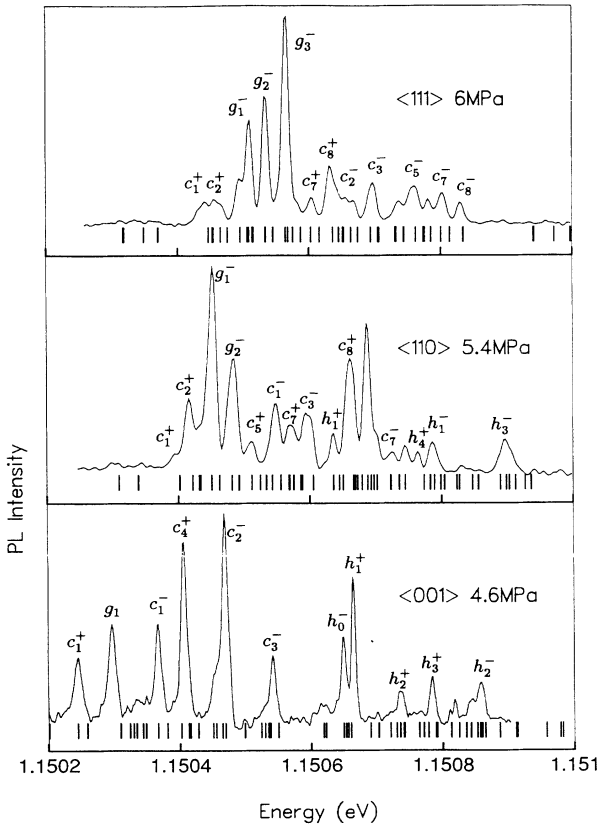

FIG. 2. Boron BE no-phonon photoluminescence spectra at moderate stress in three directions at 2 K. Lines corresponding to transitions from the BE ground state are labeled g, those from "cold" valleys (electron energy lowered by stress) are labeled c, and those from a "hot" valley (electron energy raised by stress) are labeled h. Subscripts + and − show the final state of the transition as $|m_j| = \frac{3}{2}$ or $|m_j| = \frac{1}{2}$, respectively. Tick marks show theoretical predictions. The spectra were measured at 2 K.

IV. THEORETICAL FRAMEWORK

The shell model (SM),[18] including the predictions it makes for BE's under stress,[23] will be used throughout this section.

In the absence of external perturbations, the electron and the two holes move in a potential of tetrahedral symmetry (T_d) around the substitutional impurity site. The BE wave function is an antisymmetrized product of these three single-particle functions. We will construct a perturbation matrix to describe correlations, valley-orbit splittings, and uniaxial strain effects, using the symmetry of the single-particle states. The magnitudes of the perturbations will be described by a small number of parameters, which will be determined later from the experimental data.

The wave function of the electron can be expressed

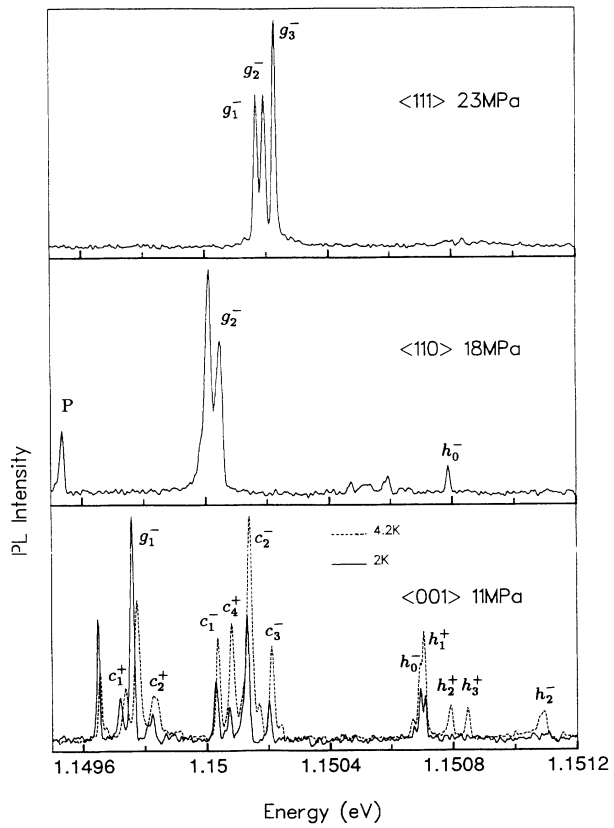

FIG. 3. Boron BE no-phonon photoluminescence spectra at 2 K under ⟨001⟩, ⟨110⟩, and ⟨111⟩ uniaxial stress. P indicates a transition of the phosphorus BE; other labels are as in Fig. 2. For ⟨001⟩ stress the broken line shows the spectrum at 4.2 K, indicating changes in initial-state populations. The small energy shifts between the 2- and 4.2-K spectra are not due to temperature, but rather a small difference in the stress.

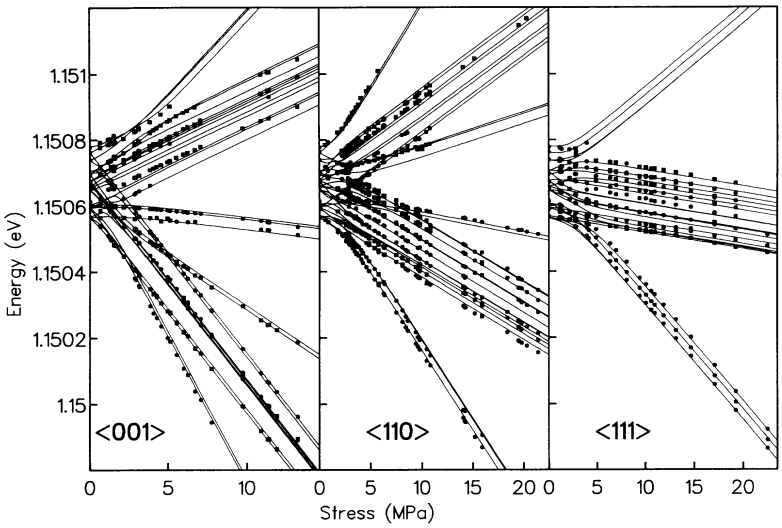

FIG. 4. Energy levels of the boron BE under ⟨001⟩, ⟨110⟩, and ⟨111⟩ stress, obtained by adding (squares) or subtracting (circles) half of the boron acceptor splitting to the observed photon energies. The lines show theoretical predictions.

as a product of a spinor, Γ_6, and a spatial part $O_m = F_m(r)u_m(r)$, the product of a smooth envelope function, $F_m(r)$, and the Bloch function of the mth conduction-band minimum, $u_m(r)$. Valley-orbit states having Γ_1, Γ_3, and Γ_5 symmetry are formed by linear combinations[18,23,34] of the O_m:

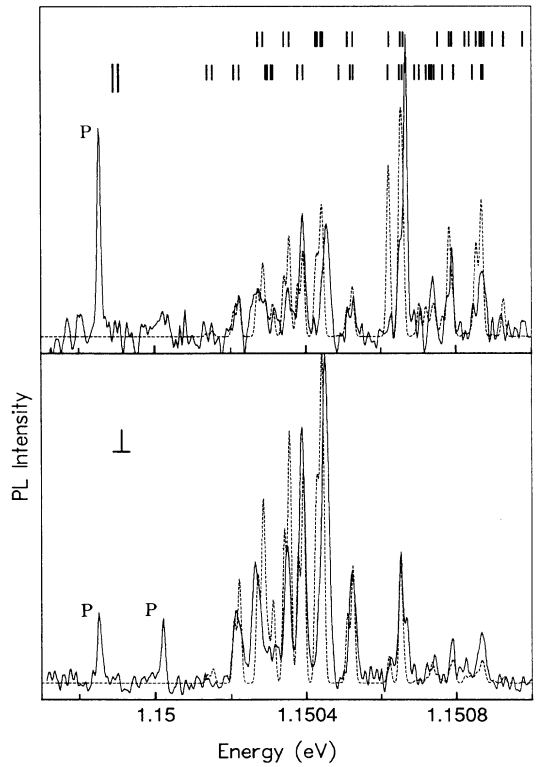

FIG. 5. Polarized spectra measured at 2 K of the boron BE under 5 MPa ⟨001⟩ stress compared with theoretical predictions (broken line). The luminescence is polarized with its electric vector parallel to the stress in the upper spectrum, and perpendicular to the stress in the lower one. P indicates a transition of the phosphorus BE.

$$\Phi_i(r) = \sum_{m=1}^{6} \alpha_{im} O_m \quad (i = 1, \ldots, 6), \tag{4.1}$$

where the coefficients α_{im}, in terms of the six equivalent ⟨111⟩ minima, are

$$\alpha_{\Gamma_1} = \frac{1}{\sqrt{6}}(1,1,1,1,1,1), \qquad i = 1,$$

$$\alpha_{\Gamma_3} = \begin{cases} \frac{1}{\sqrt{12}}(-1,-1,-1,-1,2,2), & i = 2 \\ \frac{1}{2}(1,1,-1,-1,0,0), & i = 3, \end{cases} \tag{4.2}$$

$$\alpha_{\Gamma_5} = \begin{cases} \frac{1}{\sqrt{2}}(1,-1,0,0,0,0), & i = 4 \\ \frac{1}{\sqrt{2}}(0,0,1,-1,0,0), & i = 5 \\ \frac{1}{\sqrt{2}}(0,0,0,0,1,-1), & i = 6. \end{cases}$$

The valley-orbit splitting, in any basis, can be described by two parameters, Δ_1 and Δ_3, equal to the differences in energy between Γ_1 and Γ_5, and between Γ_3 and Γ_5, respectively.

In the present work it is more convenient to take the O_m states as the basis states, rather than the Φ_i used to describe the behavior of the electron. Then the valley-orbit splitting matrix has the form

$$H^{vo} = \begin{pmatrix} d_1 & d_1 & d_2 & d_2 & d_2 & d_2 \\ d_1 & d_1 & d_2 & d_2 & d_2 & d_2 \\ d_2 & d_2 & d_1 & d_1 & d_2 & d_2 \\ d_2 & d_2 & d_1 & d_1 & d_2 & d_2 \\ d_2 & d_2 & d_2 & d_2 & d_1 & d_1 \\ d_2 & d_2 & d_2 & d_2 & d_1 & d_1 \end{pmatrix}, \tag{4.3}$$

where $d_1 = (\Delta_1 + 2\Delta_3)/6$ and $d_2 = (\Delta_1 - \Delta_3)/6$.

Under ⟨111⟩ uniaxial stress the conduction band does not split, so the electron-stress component of the Hamiltonian $H^{es} = 0$. For ⟨001⟩ and ⟨110⟩ uniaxial compression, the valleys on the z axis split from the x and y valleys, becoming lower in energy under ⟨001⟩ compression and higher under ⟨110⟩ compression. The splittings can be described by the same matrix:

$$H^{es} = \begin{pmatrix} E_x & 0 & 0 & 0 & 0 & 0 \\ 0 & E_{\bar{x}} & 0 & 0 & 0 & 0 \\ 0 & 0 & E_y & 0 & 0 & 0 \\ 0 & 0 & 0 & E_{\bar{y}} & 0 & 0 \\ 0 & 0 & 0 & 0 & E_z & 0 \\ 0 & 0 & 0 & 0 & 0 & E_{\bar{z}} \end{pmatrix}. \tag{4.4}$$

Here the energy perturbations $E_x, \ldots, E_{\bar{z}}$ are given in terms of the strain tensor components ϵ_{ij} and deformation potentials Ξ_d and Ξ_u by[34]

$$E_x = E_{\bar{x}} = \Xi_d \epsilon + \Xi_u \epsilon_{xx},$$
$$E_y = E_{\bar{y}} = \Xi_d \epsilon + \Xi_u \epsilon_{yy},$$
$$E_z = E_{\bar{z}} = \Xi_d \epsilon + \Xi_u \epsilon_{zz},$$

where

$$\epsilon = \sum_{i=x,y,z} \epsilon_{ii}.$$

In the absence of external perturbations, holes in the BE occupy a quartet of states, derived from the angular momentum $j = \frac{3}{2}$ branch of the valence band, which transform as Γ_8 in the point group T_d. Any stress will split these states into two doublets, which can be classified by their angular momentum projection, $m_j = \pm\frac{3}{2}$ and $m_j = \pm\frac{1}{2}$, on the stress axis.

The effect of uniaxial stress on the Γ_8 hole states at the valence-band maximum can be described by the term in the Hamiltonian[34]

$$H^{hs}(\epsilon) = a\epsilon - b\sum_i (J_i^2 - \tfrac{5}{4})\epsilon_{ii} - \frac{d}{\sqrt{3}}\sum_{ij}[J_i, J_j]\epsilon_{ij}, \tag{4.5}$$

where $[J_i, J_j] = \frac{1}{2}(J_iJ_j + J_jJ_i)$. The J_i are the angular momentum projection operators and a, b, and d are deformation potentials for the boron BE, which may not be the same as those for the valence band.

To describe the hole-hole and electron-hole interaction Hamiltonians, H^{hh} and H^{ehh}, we will use the basis

$$\Psi_{mpij} = O_m \sigma_p \psi_{ij}, \tag{4.6}$$

where the indices are $m = 1, \ldots, 6$, $i < j = 1, \ldots, 4$, and $p = 1, 2$; σ_p is the spinor part of the electron wave function, and $\psi_{ij} = \{\phi_i, \phi_j\}$ is the antisymmetrized product of the two one-hole wave functions, ϕ_i and ϕ_j, in the basis Γ_8.

We can use the method of invariants, developed by Bir and Pikus,[35] to construct the matrices H^{hh} and H^{ehh} from a linear combination of matrices which are invariant under T_d symmetry transformations, acting on the basis functions of Eq. (4.6). This gives N_0 linearly independent invariant matrices in each term:

$$N_0 = \frac{1}{2h}\sum_g \chi_\kappa(g)[\chi_\nu^2(\hat{g}) \pm \chi_\nu(g^2)], \tag{4.7}$$

where h is the order of group T_d, χ_κ and χ_ν are the characters of the representations D_κ of the perturbation operator (here Γ_1, symmetric under time inversion), and D_ν of the basis function. (The + applies if the representation D_ν is normal, the − if it is a spinor representation.)

The hole-hole interaction matrix H^{hh} is then given by the direct product of a matrix written in the basis of the two-hole functions, ψ_{ij}, and the unit matrix, in the basis of the electron functions, $O_m\sigma_p$. Since

$$D_\nu = \{\Gamma_8 \otimes \Gamma_8\} = \Gamma_1 + \Gamma_3 + \Gamma_5,$$

H^{hh} is comprised of three independent operators, including the unit operator (which merely changes the origin of the energy and so is omitted here):

$$H^{hh} = C_1^{hh}\sum_{i=x,y,z} J_{1i}J_{2i} + C_2^{hh}\sum_{i=x,y,z}(J_{1i}^3J_{2i} + J_{1i}J_{2i}^3). \tag{4.8}$$

J_{1i} and J_{2i} act on the first and second hole coordinates. The two terms in Eq. (4.8) describe **j-j** coupling. The first term represents the spherical approximation, which splits the Γ_1 from the degenerate Γ_3 and Γ_5 states; the second term represents the cubic correction to it, giving the three states Γ_1, Γ_3, and Γ_5.

In the case of H^{ehh} the reducible representation D_ν becomes that of the product of the electronic orbital, spin, and hole states:

$$D_\nu = (\Gamma_1 + \Gamma_3 + \Gamma_5) \otimes \Gamma_6 \otimes \{\Gamma_8 \otimes \Gamma_8\} = 6\Gamma_6 + 6\Gamma_7 + 12\Gamma_8 \tag{4.9}$$

and $N_0 = 120$. We will simplify it by making two assumptions.

(i) The electron interacts with each of the two holes separately, which means that the matrix elements

$$\langle mpij|H^{ehh}|nqkl\rangle$$

in the basis of Eq. (4.6), $O_m\sigma_p\psi_{ij}$, can be constructed from the electron–single-hole matrix elements $\langle mpi|H^{eh}|nqk\rangle$ in the basis of functions $O_m\sigma_p\phi_i$:[36]

$$\begin{aligned}\langle mpij|H^{ehh}|nqkl\rangle = {} & \langle mpi|H^{eh}|nqk\rangle\delta_{jl} \\ & + \langle mpj|H^{eh}|nql\rangle\delta_{ik} \\ & - \langle mpi|H^{eh}|nql\rangle\delta_{jk} \\ & - \langle mpj|H^{eh}|nqk\rangle\delta_{il},\end{aligned} \tag{4.10}$$

where $\delta_{ij} = 1$ if $i = j$ and 0 otherwise.

(ii) The matrix elements of H^{eh} are zero between different single valley functions. Consequently, although thermalization can occur between different valley states (Fig. 3), we will assume that there is a negligible effect on the energy levels from the electron-hole interaction scattering the electron from one valley to another.

With the second assumption H^{eh} can be expressed in block diagonal form, with each block corresponding to one of the electron valley states:

$$H^{eh} = \begin{pmatrix} H_x^{eh} & 0 & 0 & 0 & 0 & 0 \\ 0 & H_{\bar{x}}^{eh} & 0 & 0 & 0 & 0 \\ 0 & 0 & H_y^{eh} & 0 & 0 & 0 \\ 0 & 0 & 0 & H_{\bar{y}}^{eh} & 0 & 0 \\ 0 & 0 & 0 & 0 & H_z^{eh} & 0 \\ 0 & 0 & 0 & 0 & 0 & H_{\bar{z}}^{eh} \end{pmatrix}. \tag{4.11}$$

Each block H_i^{eh} on the diagonal is a 12 × 12 matrix derived from the two holes in the fourfold-degenerate $j = \frac{3}{2}$ states (giving six states after allowing for the Pauli exclusion principle), combined with the two electron-spin states. We can use the method of invariants to construct H_z^{eh}, and the other blocks are derived by simple rotations of H_z^{eh}.

An electron in the z valley has the point group C_{2v}, obtained by imposing a z axis on the T_d group. In C_{2v}, the holes transform as $D_\nu = 3\Gamma_1+\Gamma_2+\Gamma_3+\Gamma_4$, and with the electron spin (as Γ_5), $N_0 = 12$, including the unit matrix. If we assume that the central cell potential has very little effect on the electron-hole interaction, C_{4v} (a subgroup of the O_h cubic group) can be used to represent the z electron valley. In this higher group, the interaction matrix is simply reduced to[37]

$$H_z^{eh} = C_1^{eh}(J_x \otimes S_x + J_y \otimes S_y + J_z \otimes S_z) + C_2^{eh}(J_x^3 \otimes S_x + J_y^3 \otimes S_y + J_z^3 \otimes S_z) + C_3^{eh}(J_z \otimes S_z) + C_4^{eh}(J_z^3 \otimes S_z) C_5^{eh}(V_x \otimes S_x - V_y \otimes S_y) + C_6^{eh}(J_z^2 - \tfrac{5}{4}I), \quad (4.12)$$

where $V_x = [J_x, (J_y^2 - J_z^2)]$, $V_y = [J_y, (J_z^2 - J_x^2)]$, and the unit matrix has not been included explicitly. The first and second terms in Eq. (4.12) describe the electron-hole interaction in the spherical approximation, and corrections for the cubic part of the hole wave function. The third, fourth, and fifth terms correct for the anisotropy of the electron wave function. The sixth term takes into account the Coulomb interaction of the electron and a hole with anisotropic wave functions, i.e., crystal splitting.[38]

The energy levels of the boron BE can then be obtained from the solution of the secular equation

$$\det(H - \lambda I) = 0, \quad (4.13)$$

where I is the unit matrix and H is the total perturbation matrix, given by Eqs. (4.3), (4.4), (4.5), (4.8), and (4.12) as the 72 × 72 matrix:

$$H = H^{hh} + H^{ehh} + H^{\rm vo} + H^{\rm hs} + H^{\rm es}. \quad (4.14)$$

The photoluminescence spectra show photon transitions from these states to the ground state of the boron acceptor. The final state is split into two components under stress corresponding to the projection of the hole angular momentum on the stress axis of $m_j = \pm\frac{3}{2}$ (the upper level) and $m_j = \pm\frac{1}{2}$ (the lower level). To compare theoretical energies with the experimental spectra this splitting must be included.

The eigenvectors of the matrix H, corresponding to each of the eigenvalues λ in Eq. (4.13), give the wave functions of each of the BE states. Using these, it is possible to predict the intensities of the spectral lines. A transition between the nth BE state

$$E^n = \sum_{m,p,i,j} c_{mpij}^n O_m \sigma_p \psi_{ij}$$

and single hole state ψ_k has intensity in the $\underline{e}$ polarization given by

$$I(n,k,\underline{e}) \propto |\langle E^n|\underline{e}|\psi_k\rangle|^2, \quad (4.15)$$

where the electric vector of the light has a direction $\underline{e}$. We can evaluate these matrix elements:

$$\langle E^n|\underline{e}|\psi_k\rangle = \sum_{mpij} c_{mpij}^n (p_{mpi}^{\underline{e}}\delta_{ik} - p_{mpj}^{\underline{e}}\delta_{jk}), \quad (4.16)$$

where $p_{mpi}^{\underline{e}}$ is the single electron-hole matrix element given by Gorbunov *et al.*[27] in terms of parameters η, λ, and γ, for polarization $\underline{e}$. Thermalization between states is included by a Boltzmann factor $e^{-\varepsilon_n/kT}$ for a state with energy ε_n at temperature T.

V. DISCUSSION

In contrast to other group-III acceptors in Si, in which the hole-hole interactions are much larger, for boron the hole-hole and electron-hole interactions have comparable strengths. Consequently, at zero stress, the eigenstates are complicated admixtures of the basis states. However, the magnitudes of the valley-orbit splitting can be determined directly from experiment by using the data for large ⟨111⟩ compressions.

In the limit of high stress, the dominant splitting of the hole states is into two doubly degenerate levels with angular momentum projected along the stress axis, described by quantum numbers $m_j = \pm\frac{3}{2}$ and $\pm\frac{1}{2}$. Under compression, the $m_j = \pm\frac{1}{2}$ states have the lower (hole) energy. In this case the antisymmetrized product of the two hole states transforms according to the unit representation Γ_1 and there is no splitting produced by the hole-hole interaction [Eq. (4.8)] or the electron-hole interaction [Eq. (4.12)]. Under ⟨111⟩ stress, there is no splitting of the conduction-band minima. Consequently, as was pointed out by Karasyuk and Pokrovskii,[30] the spectra recorded under large ⟨111⟩ compressive stress (Fig. 3) give the magnitudes of the valley-orbit splittings immediately, from the splitting of the lowest-energy triplet, as

$$\Delta_1 = 32\ \mu\text{eV}, \qquad \Delta_3 = -26\ \mu\text{eV}, \quad (5.1)$$

where Δ_1 is the energy difference between Γ_1 and Γ_5 and Δ_3 is that between Γ_3 and Γ_5.

A least-squares-fit algorithm was used to minimize the

TABLE I. Interaction constants C_i^{hh} and C_j^{eh} (μeV).

C_1^{hh}	C_2^{hh}	C_1^{eh}	C_2^{eh}	C_3^{eh}	C_4^{eh}	C_5^{eh}	C_6^{eh}
-111	27	-37	19	-37	9	14	-16

TABLE II. Deformation constants (eV).

Defect	b	d	Ξ_u
Boron BE	-1.49±0.05	-4.08±0.1	8.5±0.2
Boron acceptor	-1.35±0.05	-3.95±0.1	
Phosphorus BE	-1.72±0.05	-4.53±0.1	

difference between the theoretically predicted and experimentally observed energy levels both at zero and high stress perturbations for all three directions of stress. In the fit, Δ_1 and Δ_3 were fixed at the values of Eq. (5.1), and we varied the hole-hole parameters C_1^{hh},C_2^{hh}, the six electron-hole parameters $C_1^{eh},\ldots,C_6^{eh}$, the electron deformation parameter Ξ_u, the hole deformation parameters b, d and slope and shift parameters (which included the hydrostatic component and the unit matrix terms ignored earlier). The values of the best-fitting interaction parameters are given in Table I, and the deformation parameters are given in Table II. Figure 4 shows the energy of the boron BE under stress, with the final-state splitting taken into account, along with the corresponding theoretical energies. The agreement is excellent.

Spectra recorded with the electric vector of the luminescence nominally parallel and perpendicular to the applied stress of 5 MPa along ⟨001⟩ are shown in Fig. 5. The broken lines show the theoretical predictions, using the parameters of Table I. We assumed a Gaussian line shape of a width similar to that observed, some mixing of polarizations in the experimental data, and used values of the further parameters η, λ, and γ in the one-electron–hole matrix elements in Gorbunov's paper,[27] obtained in a similar way to his. Thermalization between all the initial states has been included, with an assumed temperature of 2 K. The satisfactory agreement between the measured and calculated spectra confirm that the theory developed here is valid.

VI. CONCLUSIONS

Our investigation of the boron-bound-exciton fine structure under stress has shown that there is a large number of energy levels which appear in the no-phonon photoluminescence as very narrow spectral components. We have developed a full theoretical treatment of the BE under uniaxial stress, and have applied it to account, in detail, for the very complex splittings of components seen in the spectra. The excellent fit between the experimental data and theoretical predictions of both the fan diagrams and the spectra themselves demonstrate that the assumptions used in the theoretical model were justified.

The hole-hole interaction parameters C_1^{hh} and C_2^{hh} are very much smaller, at −111 and 27 μeV, respectively, for boron than for the other acceptors in silicon. Using the reported hole-hole splittings for the other acceptors,[39] we calculate the C_1^{hh} terms to be 750 μeV for Al, 1050 μeV for Ga, and 5700 μeV for In. Similarly, the C_2^{hh} terms are −100 μeV for Al, −150 μeV for Ga, and −1030 μeV for In. For B there is a near cancellation of the effects of the C_1^{hh} and C_2^{hh} terms, resulting in very small splittings. Moving through the sequence of the acceptors we see that these interactions change, as is qualitatively expected, with increasing hole binding energy; the spherical term C_1^{hh} increases as does the magnitude of the cubic correction term C_2^{hh}. The electron-hole interaction terms $C_1^{eh},\ldots,C_6^{eh}$ reported here are not available for other acceptor BE's in silicon, and so we are unable to make comparisons between the acceptors. For the valley-orbit splitting, our values for B of Δ_1=32 μeV and Δ_3=−26 μeV compare with Δ_1=83 μeV,Δ_3=−25 μeV for Al and Δ_1=13 μeV,Δ_3=−29 μeV for Ga,[27] with the same order of the levels: Γ_3, Γ_5, Γ_1.

Localization of the exciton on a boron acceptor reduces its crystal splitting to $2C_6^{eh}$=38 μeV (Table I) from the free-exciton value, which derives from the anisotropy of the conduction-band minima of 0.31 meV.[40] However, our analysis shows that the central cell effects have very little influence on the correlations between the electrons and holes in the bound exciton. We have also been able to ignore the effects on the stress-splitting patterns of intervalley scattering by the electron-hole interactions. Weak scattering does occur, however, as shown by the thermalization of the stress-split components. Finally, the deformation constants for holes in the boron BE are shown in Table II to be very similar to the values for the hole at the neutral acceptor.

In this paper we have presented data for the exciton bound at a boron acceptor at a high level of refinement. There is a need to carry out similar work on the other acceptors, particularly as the ultrahigh-resolution spectra of these show additional structure in the absence of external perturbations, which has not yet been explained.[4]

ACKNOWLEDGMENTS

The authors are grateful to T. W. Steiner, D. J. S. Beckett, and M. K. Nissen from Simon Fraser University for their assistance. This work was supported, partly, by NSERC (Canada), SERC (U.K.), and the Leverhulme Trust (U.K.).

*On leave of absence from The Institute of Radioengineering and Electronics, Academy of Sciences of the U.S.S.R., 18 Marx Avenue, Moscow 103907, U.S.S.R. Present address: Department of Physics, Simon Fraser University, Burnaby, British Columbia, Canada V5A 1S6.

†Present address: Institute for Microstructural Sciences, National Research Council Canada, Ottawa, Canada K1A 0R6.

[1] J. R. Haynes, Phys. Rev. Lett. **2**, 256 (1960).
[2] P. J. Dean, J. R. Haynes, and W. F. Flood, Phys. Rev. **161**, 711 (1967).
[3] M. Tajima, Appl. Phys. Lett. **35**, 719 (1978).
[4] H. Nakayama, T. Nishino, and Y. Hamakawa, Jpn. J. Appl. Phys. **19**, 501 (1980).
[5] A. S. Kaminskii, L. I. Kolesnik, B. M. Leiferov, and Ya. E. Pokrovskii, Zh. Prikl. Spektrosk. **36**, 745 (1982) [J. Appl. Spectrosc. (USSR) **36**, 516 (1982)].
[6] P. McL. Colley and E. C. Lightowlers, Semicond. Sci. Technol. **2**, 157 (1987).
[7] P. J. Dean, W. F. Flood, and G. Kaminsky, Phys. Rev. **163**, 721 (1967).
[8] M. A. Vouk and E. C. Lightowlers, J. Lumin. **15**, 357 (1977).
[9] M. L. W. Thewalt, G. Kirczenow, R. R. Parsons, and R. Barrie, Can. J. Phys. **54**, 1728 (1976).
[10] A. S. Kaminskii, Ya. E. Pokrovskii, and N. V. Alkeev, Zh. Eksp. Teor. Fiz. **59**, 1937 (1970) [Sov. Phys.—JETP **32**, 1048 (1971)].
[11] R. Sauer, Phys. Rev. Lett. **31**, 376 (1973).
[12] K. Kosai and M. Gershenzon, Phys. Rev. B **9**, 723 (1974).
[13] R. Sauer and J. Weber, Phys. Rev. Lett. **36**, 48 (1976).
[14] For a review of BE and BMEC in Si to 1980, see M. L. W. Thewalt, in *Excitons*, edited by E. I. Rashbo and M. D. Sturge (North-Holland, Amsterdam, 1982), pp. 393–458.
[15] M. L. W. Thewalt, Phys. Rev. Lett. **38**, 521 (1977).
[16] E. C. Lightowlers and M. O. Henry, J. Phys. C **10**, L247 (1977).
[17] S. A. Lyon, D. L. Smith, and T. C. McGill, Phys. Rev. B **17**, 2620 (1978).
[18] G. Kirczenow, Can. J. Phys. **55**, 1787 (1977).
[19] G. F. Koster, J. O. Dimmock, R. G. Wheeler, and H. Statz, *Properties of the Thirty-two Point Groups* (MIT Press, Cambridge, MA, 1966).
[20] V. D. Kulakovskii and A. V. Malyavkin, Phys. Status Solidi B **92**, 455 (1979).
[21] A. S. Kaminskii, V. A. Karasyuk, and Ya. E. Pokrovskii, Zh. Eksp. Teor. Fiz. **74**, 2234 (1978) [Sov. Phys.—JETP **47**, 1162 (1978)].
[22] V. D. Kulakovskii, Fiz. Tverd. Tela (Leningrad) **20**, 1394 (1978) [Sov. Phys.—Solid State **20**, 802 (1978)].
[23] M. L. W. Thewalt, J. A. Rostworowski, and G. Kirczenow, Can. J. Phys. **57**, 1898 (1979).
[24] R. R. Parsons, Solid State Commun. **22**, 671 (1977).
[25] A. S. Kaminskii, V. A. Karasyuk, and Ya. E. Pokrovskii, Zh. Eksp. Teor. Fiz. **79**, 422 (1980) [Sov. Phys.—JETP **52**, 211 (1980)].
[26] A. S. Kaminskii, V. A. Karasyuk, and Ya. E. Pokrovskii, Zh. Eksp. Teor. Fiz. **83**, 2237 (1982) [Sov. Phys.—JETP **56**, 1295 (1983)].
[27] M. V. Gorbunov, A. S. Kaminskii, and A. N. Safanov, Zh. Eksp. Teor. Fiz. **94**, 247 (1988) [Sov. Phys.—JETP **67**, 355 (1988)].
[28] A. S. Kaminskii and A. N. Safonov, Fiz. Tverd. Tela (Leningrad) **31**, 100 (1989) [Sov. Phys.—Solid State **31**, 971 (1989)].
[29] M. L. W. Thewalt, Can. J. Phys. **55**, 1463 (1977).
[30] V. A. Karasyuk and Ya. E. Pokrovskii, Pis'ma Zh. Eksp. Teor. Fiz. **37**, 537 (1983) [JETP Lett. **37**, 640 (1983)].
[31] M. L. W. Thewalt, M. K. Nissen, D. J. S. Beckett, and K. R. Lundgren, in *Impurities, Defects and Diffusion in Semiconductors: Bulk and Layered Structures*, edited by D. J. Wolford, J. Bernholc, and E. E. Haller, MRS Symposia Proceedings No. 163 (Materials Research Society, Pittsburgh, 1990), p. 221.
[32] M. L. W. Thewalt and D. M. Brake, Mater. Sci. Forum **65-66**, 187 (1990).
[33] V. A. Karasyuk, E. C. Lightowlers, M. L. W. Thewalt, A. G. Steele, and D. M. Brake, Mater. Sci. Forum **65**, 205 (1990).
[34] A. K. Ramdas and S. Rodrigues, Rep. Prog. Phys. **44**, 1297 (1981).
[35] G. L. Bir and G. E. Pikus, *Simmetrya i Deformatsionnye Effecty v Poluprovodnikakh* (Izdatel'stvo "Nauka," Moscow, 1972) [*Symmetry and Strain-Induced Effects in Semiconductors* (Halsted, New York, 1974)].
[36] E. U. Condon and G. H. Shortley, *The Theory of Atomic Spectra* (Cambridge University Press, Cambridge, 1964).
[37] V. A. Kaminskii, V. A. Karasyuk, and Ya. E. Pokrovskii, Zh. Eksp. Teor. Fiz. **83**, 2237 (1982) [Sov. Phys.—JETP **56**, 1295 (1983)].
[38] G. E. Pikus, Fiz. Tverd. Tela (Leningrad) **19**, 1653 (1977) [Sov. Phys.—Solid State **19**, 965 (1977)].
[39] K. R. Elliott, G. C. Osbourn, D. L. Smith, and T. C. McGill, Phys. Rev. B **17**, 1808 (1978).
[40] R. B. Hammond and R. N. Silver, Solid State Commun. **28**, 993 (1978).